

Noncovalent and site-directed spin labeling of duplex RNA

Nilesh R. Kamble,¹ Markus Gränz,² Thomas F. Prisner² and Snorri Th. Sigurdsson*¹

¹University of Iceland, Department of Chemistry, Science Institute, Dunhaga 3, 107 Reykjavik, Iceland.

²Institute of Physical and Theoretical Chemistry and Center of Biomolecular Magnetic Resonance, Goethe University, Max-von-Laue-Str. 7, 60438 Frankfurt am Main, Hessen, Germany

Table of Contents

List of abbreviations	S2
Synthetic procedures	S2
General materials and methods	S2
DNA and RNA synthesis and purifications	S2
Synthesis of the spin label \dot{G}	S3
EPR measurements	S4
General	S4
Effect of the identity of the orphan base on \dot{G} -binding to an abasic site in a DNA duplex	S5
Temperature dependence of \dot{G} -binding to an abasic site in duplex RNA	S5
Effect of flanking sequence on noncovalent spin labeling of RNA with \dot{G}	S6
Determination of non-specific binding of \dot{G} to an unmodified RNA duplex	S6
Distance measurements on a noncovalently labeled RNA duplex by PELDOR	S7
Molecular modeling of \dot{G} in the 22-mer RNA duplex containing two abasic sites	S8
References	S9

List of abbreviations

DMF	<i>N,N</i> -dimethylformamide
CW	continuous-wave
EPR	electron paramagnetic resonance
HRMS-ESI	high resolution mass spectrometry-electrospray ionization
NMR	nuclear magnetic resonance
A	adenine
C	cytosine
G	guanine
T	thymine
U	uracil

Synthetic procedures

General materials and methods

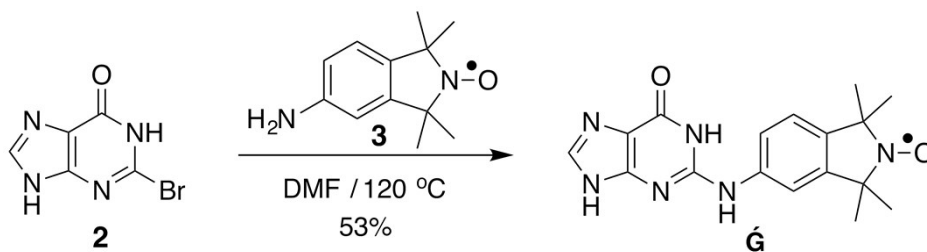
All reagents were purchased from commercial suppliers and were used without purification. Dichloromethane and acetonitrile were dried over calcium hydride and freshly distilled before use. Thin layer chromatography (TLC) was performed using glass plates pre-coated with silica gel (0.25 mm, F-25, Silicycle) and compounds were visualized by UV light. Column chromatography was performed using 230-400 mesh silica gel (Silicycle). ¹H NMR spectra were recorded with a Bruker Avance 400 MHz spectrometer. Chemical shifts were reported in parts per million (ppm) relative to the partially deuterated NMR solvent *d*₆-DMSO (2.50 ppm). Nitroxide radicals show significant broadening in NMR spectra and loss of NMR signals due to their paramagnetic nature.^{1, 2} Mass spectrometric analysis were performed on an HR-ESI-MS (Bruker, MicroTOF-Q) in positive ion mode. All EPR data were recorded in a phosphate buffer (10 mM NaHPO₄, 100 mM NaCl, 0.1 mM Na₂EDTA; pH 7) containing 30% ethylene glycol and 2% DMSO.

DNA and RNA synthesis and purifications

All commercial phosphoramidites, CPG columns, 5-benzylthiotetrazole and acetonitrile for oligomer synthesis were purchased from ChemGenes Corp., USA. All other required reagents and solvents were purchased from Sigma-Aldrich Co. Unmodified oligonucleotides and oligonucleotides containing abasic sites were synthesized on an automated ASM800 DNA synthesizer (Biosset, Russia) using a trityl-off protocol and commercially available phosphoramidites with standard protecting groups on 1.0 μmole scale (1000 Å CPG columns). The oligomers were deprotected in a 1:1 solution (2 mL) of CH₃NH₂ (8 M in EtOH) and NH₃ (33% w/w in H₂O) at 65 °C for 45 min. The solvent was removed *in vacuo* and the TBDMS-

protecting groups were removed by incubation in $\text{NEt}_3:3\text{HF}$ (600 μL) for 90 min at 55 $^\circ\text{C}$ in DMF (200 μL), followed by addition of water (200 μL). The oligonucleotides were purified by 20% denaturing polyacrylamide gel electrophoresis. The oligonucleotides were visualized by UV light and the bands were excised from the gel, crushed and extracted from the gel matrix with a Tris buffer (250 mM NaCl, 10 mM Tris, 1mM Na_2EDTA , pH 7.5). The extracts were filtered through 0.45 μm , 25 mm diameter GD/X syringe filters (Whatman, USA) and desalted using Sep-Pak cartridges (Waters, USA), according to the manufacturer's instructions. After removing the solvent *in vacuo*, the oligomers were dissolved in de-ionized and sterilized water (200 μL). Oligonucleotides were quantified using Beer's law and measurements of absorbance at 260 nm, using extinction coefficients determined by using the WinLab oligonucleotide calculator (V2.85.04, PerkinElmer).

Synthesis of the spin label **G**



To a suspension of 2-bromo-6-hydroxypurine³ (200 mg, 0.23 mmol) in DMF (5 mL) was added 1,1,3,3-tetramethylisoindoline-5-amino-2-oxyl⁴ (180 mg, 0.25 mmol). The mixture was heated to 120 $^\circ\text{C}$ for 12 h. The solvent was evaporated *in vacuo* and the residue was purified by flash column chromatography using a solvent gradient (0:100 to 10:90 MeOH: CH_2Cl_2 , containing 2% of NH_3) to give **G** as a yellow solid (167 mg, 53%).

^1H NMR (d_6 -DMSO): δ 1.69-1.72 (bd), 7.37 (bs), 7.75-8.00 (bs), 8.74(bs), 10.62 (bs), 12.70 (bs) ppm.

HR-ESI-MS: calculated for $\text{C}_{17}\text{H}_{19}\text{N}_6\text{O}_2$ 339.1569, found 340.1630 (M+1).

EPR measurements

General

Solutions for CW-EPR experiments were prepared by mixing aliquots of stock solutions of a single-stranded oligomer containing an abasic site, its complementary strand and the spin label \dot{G} (1:1.2:0.5). The solvent was evaporated *in vacuo* and the resulting residue was dissolved in phosphate buffer (10 μ L; 10 mM NaHPO₄, 100 mM NaCl, 0.1 mM Na₂EDTA, pH 7.0) and annealed: 90 °C for 2 min, 60 °C for 5 min, 50 °C for 5 min, 22 °C for 15 min and dried using a SpeedVac. The residue was dissolved in an aqueous 30% ethylene glycol solution (10 μ L) containing 2% DMSO and placed in a 50 μ L quartz capillary (BLAUBRAND intraMARK) (final concentration of nucleic acid duplex 200 μ M). The EPR spectra were recorded using 100-200 scans on a MiniScope MS200 (Magnettech Germany) spectrometer (100 kHz modulation frequency, 1.0 G modulation amplitude and 2.0 mW microwave power). Magnettech temperature controller M01 (\pm 0.5 °C) was used as temperature regulator.

For PELDOR measurements 20 μ L of sample volume with 80% buffer/20% glycerol was transferred into 1.6 mm outer diameter quartz EPR tubes (Suprasil, Wilmad LabGlass). Pulsed EPR data were recorded on an ELEXSYS E580 EPR spectrometer (Bruker) equipped with a PELDOR unit (E580-400U, Bruker), a continuous-flow helium cryostat (CF935, Oxford Instruments) and a temperature control system (ITC 502, Oxford Instruments). X-band frequency (9.4 GHz) experiments were performed at 50K with a BRUKER ER4118X-MS3 resonator and a 1 kW TWT amplifier. Pulse length were 32 ns ($\pi/2$ and π) for the probe pulses and 12 ns for the pump inversion pulse. The frequency of the pump pulse was set to the maximum of the nitroxide powder spectra and the detection frequency was changed between 40-90 MHz above, respectively. The delay time between the first two pulses of the primary echo sequence was varied between 132 ns and 196 ns in 8 ns steps in order to reduce ¹H nuclear modulation contributions to the PELDOR signal. For PELDOR experiments, the dead-time free four-pulse sequence with phase-cycled $\pi/2$ -pulses was used.⁵ Primary experimental data were background-corrected by fitting an exponential decay function for division of the intermolecular contribution. The resulting form factors F(t) were fitted with a Tikhonov regularization to distance distributions with the DeerAnalysis2013 software package.⁶

Effect of the identity of the orphan base on \dot{G} -binding to an abasic site in a DNA duplex

An evaluation of binding of \dot{G} (200 μ M) to an abasic site in four DNA duplexes (400 μ M), each of which contain different bases (A, T, G and C) opposite to the abasic site, was performed by recording the CW-EPR spectra in 10 μ L phosphate buffer (10mM NaHPO₄, 100 mM NaCl, 0.1 mM Na₂EDTA, pH 7.0) containing 30% ethylene glycol and 2% DMSO at -30 °C. As expected, much less binding of \dot{G} was observed for the orphan bases A, G and T, as compared to C, which showed nearly full binding to the abasic site in the DNA duplex (**Figure S1**).

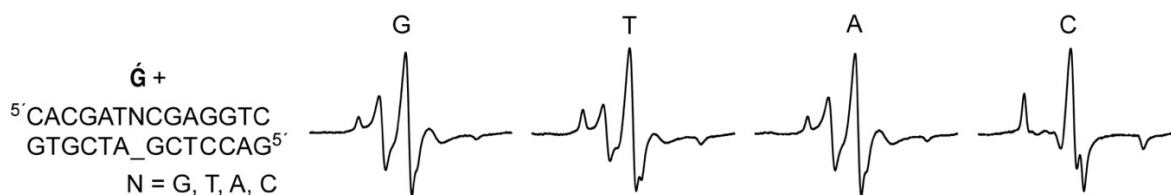


Figure S1. CW-EPR spectra of \dot{G} in the presence of DNA duplexes containing abasic sites (“_”) opposite to the four bases G, C, A and T. All EPR spectra were recorded using the same number of scans, phase corrected and aligned with respect to the height of the central peak.

Temperature dependence of \dot{G} -binding to an abasic site in duplex RNA

CW-EPR spectra of a 14-mer RNA duplex, containing an abasic site, were recorded in the presence of \dot{G} at different temperatures. Upon lowering the temperature, the amount of non-bound \dot{G} decreased, as judged by the reduction of the fast-moving component of the spectrum (**Figure S2**). At -20 °C, the spin label was fully bound.

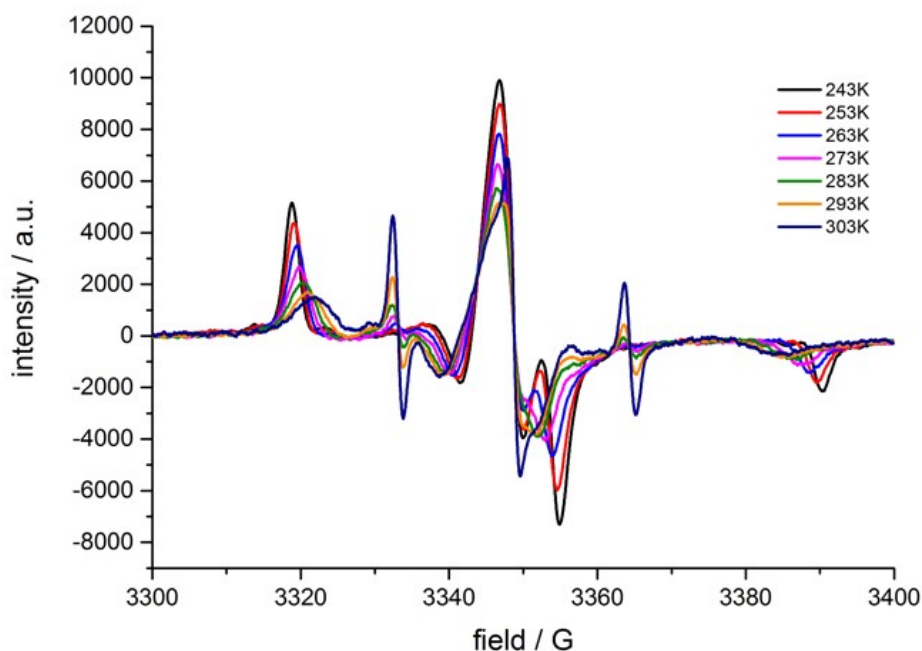


Figure S2. EPR spectra of the 14-mer RNA duplex $5' \text{CACGAUCCGAGGUC} \cdot 5' \text{GACCUCG_AUCGUG}$ as a function of temperature.

Effect of flanking sequence on noncovalent spin labeling of RNA with \dot{G} .

Stacking interaction with the flanking nucleobases presumably contribute to binding of the spin label \dot{G} to an abasic site in duplex RNA. A minor flanking sequence effect was observed when comparing purine-purine (5'-G_A), purine-pyrimidine (5'-A_U) and pyrimidine-pyrimidine (5'-C_U) base pairs immediately flanking the abasic site (Figure S2) at -20 °C. However, at -30 °C all flanking sequences showed full binding.

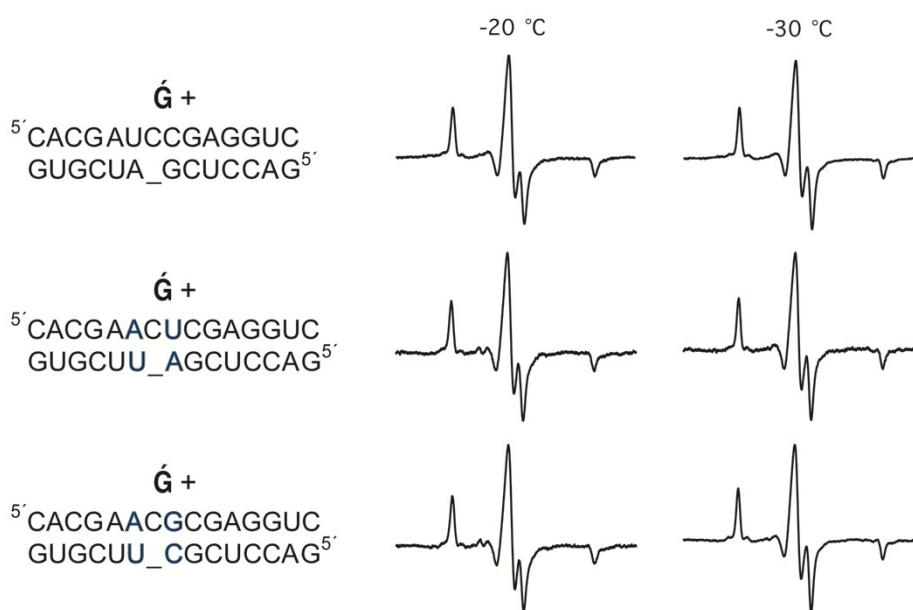


Figure S3. CW-EPR spectra of \dot{G} (200 μ M) in the presence of a duplex RNA (200 μ M) containing an abasic site () and varying flanking sequences. EPR spectra were recorded in a phosphate buffer (10 mM NaHPO₄, 100 mM NaCl, 0.1 mM Na₂EDTA, pH 7.0) containing 2% DMSO and 30% ethylene glycol.

Determination of non-specific binding of \dot{G} to an unmodified RNA duplex

The degree of non-specific binding of \dot{G} to RNA duplexes was determined by incubating \dot{G} with an unmodified RNA duplex. A 14-mer RNA duplex was mixed with one equivalent of \dot{G} and the EPR spectra were recorded at -10 °C, -20 °C and -30 °C (Figure S4). Minor non-specific binding (< 5%) was observed at -30 °C but less than 1% at -20 °C and none at -10 °C.

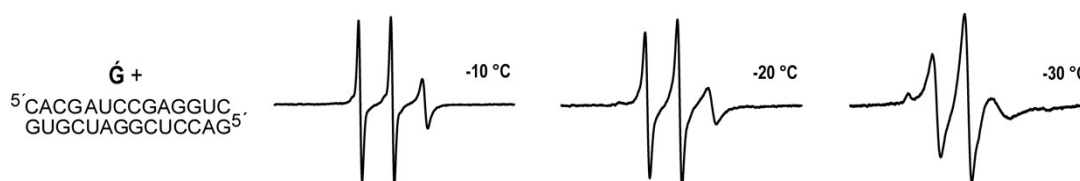


Figure S4. EPR spectra of \dot{G} (200 μ M) in the presence of an unmodified RNA (200 μ M) duplex. Measurements were recorded in a phosphate buffer (10 mM NaHPO₄, 100 mM NaCl, 0.1 mM Na₂EDTA, pH 7.0) containing 2% DMSO and 30% ethylene glycol.

The specificity of binding was also investigated by a competition experiment, in which hypoxanthine was added in varying amounts to a sample containing $\dot{\text{G}}$ (200 μM) in the presence of an RNA duplex (200 μM) containing an abasic site at 10 $^{\circ}\text{C}$. Hypoxanthine has previously been used to rescue the catalytic activity of a hammerhead ribozyme containing an abasic site.⁷ Not unexpectedly, hypoxanthine (**I**) has a lower affinity to the abasic site than $\dot{\text{G}}$, but it is clear that it is competing with $\dot{\text{G}}$ for binding to the abasic site.

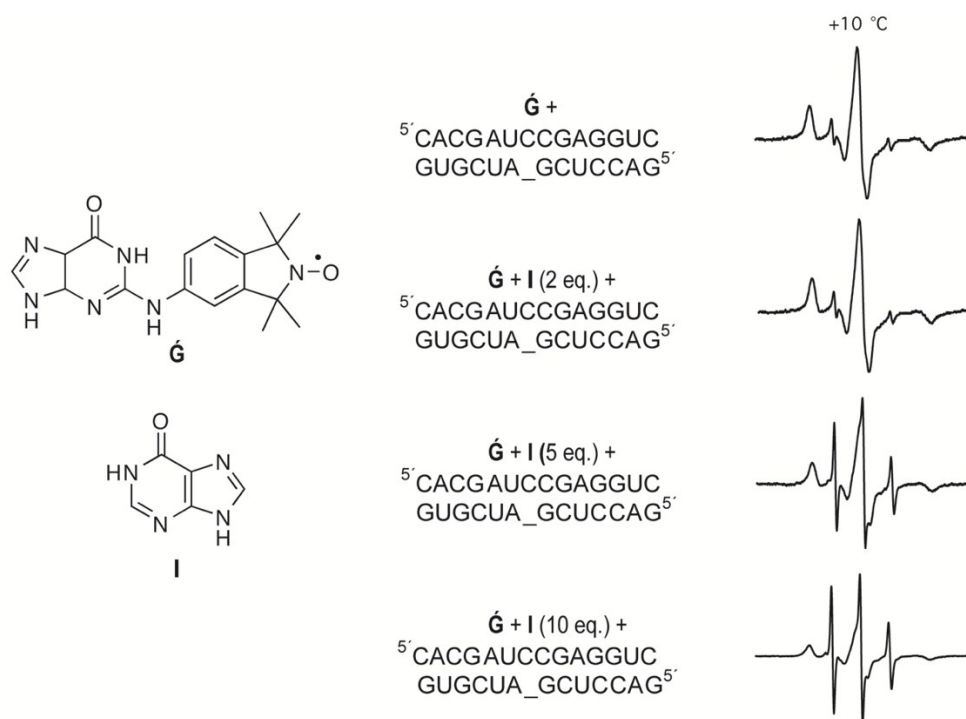


Figure S5. CW-EPR spectra of $\dot{\text{G}}$ (200 μM) in the presence of a duplex RNA (200 μM) containing an abasic site (—), along with increasing concentration of hypoxanthine (**I**) (0-10 equiv.). The EPR spectra were recorded in a phosphate buffer (10 mM NaH_2PO_4 , 100 mM NaCl , 0.1 mM Na_2EDTA , pH 7.0) containing 2% DMSO and 30% ethylene glycol.

Distance measurements on a noncovalently labeled RNA duplex by PELDOR

A duplex RNA containing two abasic sites was constructed for PELDOR measurements (**Figure S6**). Before performing the PELDOR experiment, full binding of $\dot{\text{G}}$ to both the abasic sites was verified by CW-EPR spectroscopy. The noncovalently spin-labeled 22-mer RNA duplex were prepared by mixing appropriate self-complementary single-stranded RNA (4 nmol) with one equivalent of the spin label $\dot{\text{G}}$ (4 nmol). The water/ethanol solution was evaporated *in vacuo* and the residue dissolved in a phosphate buffer. After annealing the RNA oligomer, the solvent was removed *in vacuo* and the residue dissolved in sterile water (10 μL)

containing 2% DMSO and 30% ethylene glycol. The EPR spectra were recorded (**Figure S6**) and showed full binding of \dot{G} at $-30\text{ }^{\circ}\text{C}$.

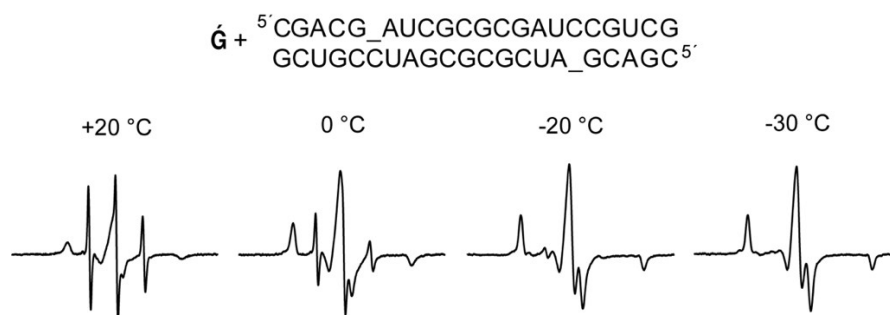


Figure S6. EPR spectra of \dot{G} (400 μM) in the presence of a 22-mer RNA duplex (200 μM) containing two abasic sites, denoted as “_”. EPR spectra were recorded in a phosphate buffer (10 mM NaHPO_4 , 100 mM NaCl , 0.1 mM Na_2EDTA , pH 7.0) containing 30% ethylene glycol and 2% DMSO.

The spin-labeled 22-mer RNA duplex was used for PELDOR measurements, using 40-90 MHz frequency offsets between the pump and probe pulses, in steps of 10 MHz. The resulting time traces with the indicated background correction (red lines) are shown in **Figure S7**.

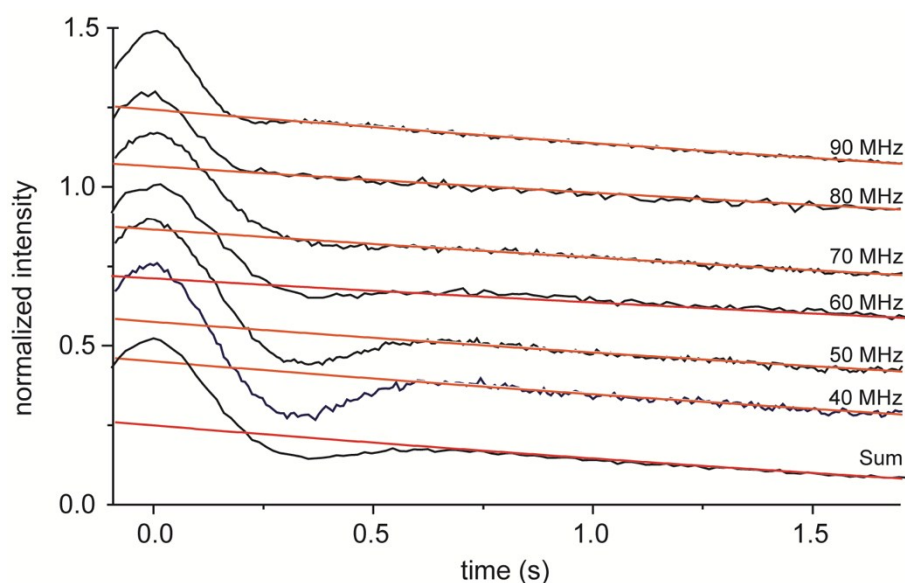


Figure S7. Original X-band PELDOR data for different offsets between the pump and probe pulses (black) along with the applied exponential background functions (red). The lowest trace shows the sum of all the frequency offsets.

Molecular modeling of \dot{G} in the 22-mer RNA duplex containing two abasic sites.

Molecular modeling was carried out on the RNA duplex in SPARTAN 10 (Wavefunction) using standard parameters. The abasic sites were generated by deleting the corresponding guanosine (G) base. The spin label \dot{G} was docked manually at the abasic sites so that it forms hydrogen bonds with the C on the opposite strand. The modeled structures were exported as

PDB files and visualized in PyMOL (Delano Scientific LCC) (**Figure S8**). Rotation of the bond between the isoindoline nitroxide and N2 of guanine in \dot{G} , yielded different conformations. **Figure S8** shows three structures resulting from two orientations of each label parallel to minor groove of the RNA. The distances between the spin labels in these three structures were measured to be 26.4 Å, 28.7 Å and 31.1 Å, yielding an average distance of 28.7 Å.

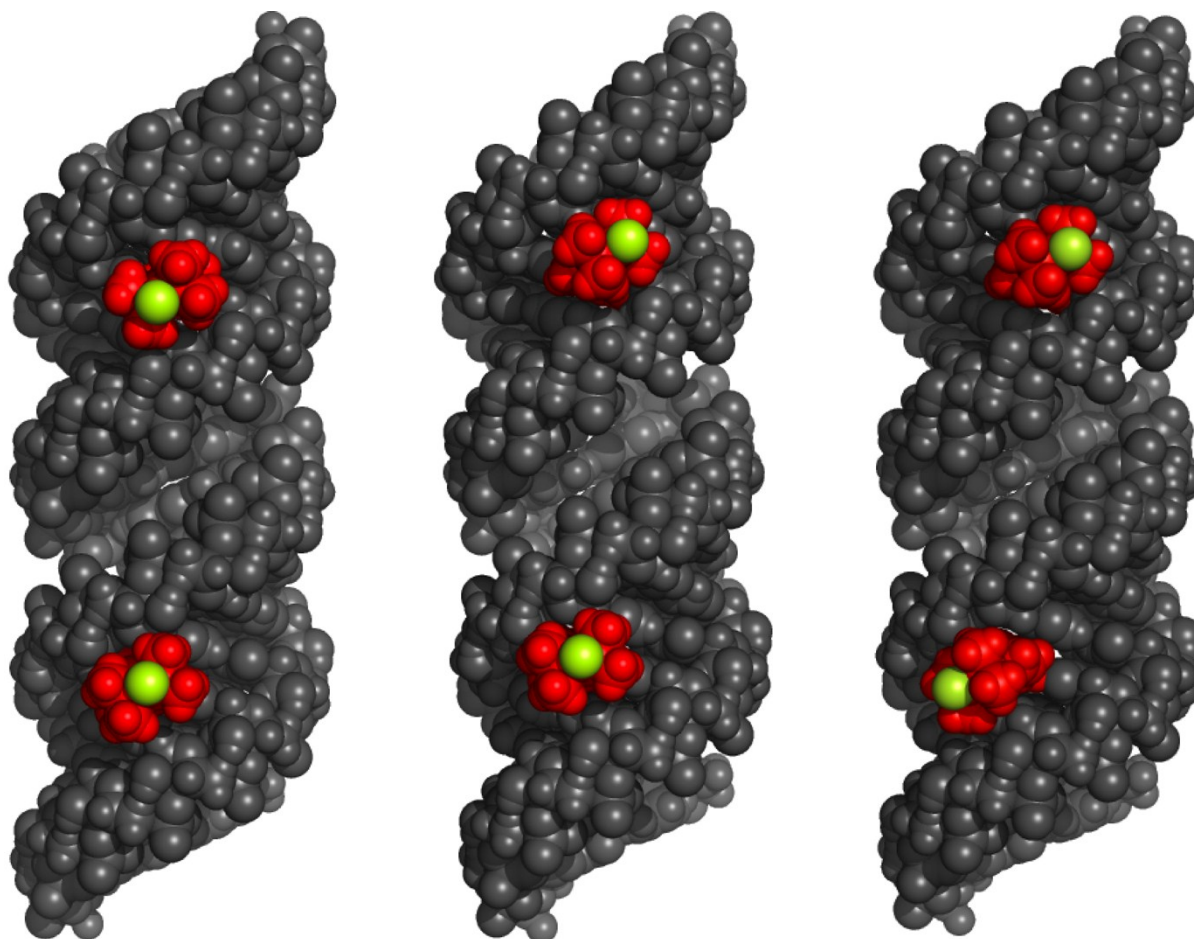


Figure S8. Molecular models of the noncovalently spin-labeled 22-mer RNA duplex in a space-filling representation showing relative position of the two \dot{G} s (red). The oxygen atoms of the nitroxide functional groups are shown in green.

References

- (1) Lee, T. D.; Keana, J. F. *Journal of Organic Chemistry* **1975**, *40* (21), 3145-3147.
- (2) Li, Y.; Lei, X.; Li, X.; Lawler, R. G.; Murata, Y.; Komatsu, K.; Turro, N. J. *Chem. Commun.* **2011**, *47* (46), 12527-12529.
- (3) Beaman, A. G.; Gerster, J. F.; Robins, R. K. *J. Org. Chem.* **1962**, *27* (3), 986-990.
- (4) Reid, D.; Bottle, S. *Chemical Communications* **1998**, (17), 1907-1908.
- (5) Pannier, M.; Veit, S.; Godt, A.; Jeschke, G.; Spiess, H. W. *Journal of Magnetic Resonance* **2011**, *213* (2), 316-325.
- (6) Jeschke, G.; Chechik, V.; Ionita, P.; Godt, A.; Zimmermann, H.; Banham, J.; Timmel, C.; Hilger, D.; Jung, H. *Applied Magnetic Resonance* **2006**, *30* (3-4), 473-498.

- (7) Peracchi, A.; Beigelman, L.; Usman, N.; Herschlag, D. *Proc. Natl. Acad. Sci. U.S.A.* **1996**, *93* (21), 11522-11527.